

Gyrokinetic Simulations of Nonlinear Tearing Instability

July 26, 2010

R. NUMATA^{A,†}, W. Dorland^A, N. F. Loureiro^B, B. N. Rogers^C, A. A. Schekochihin^D,
T. Tatsuno^A

† rnumata@umd.edu

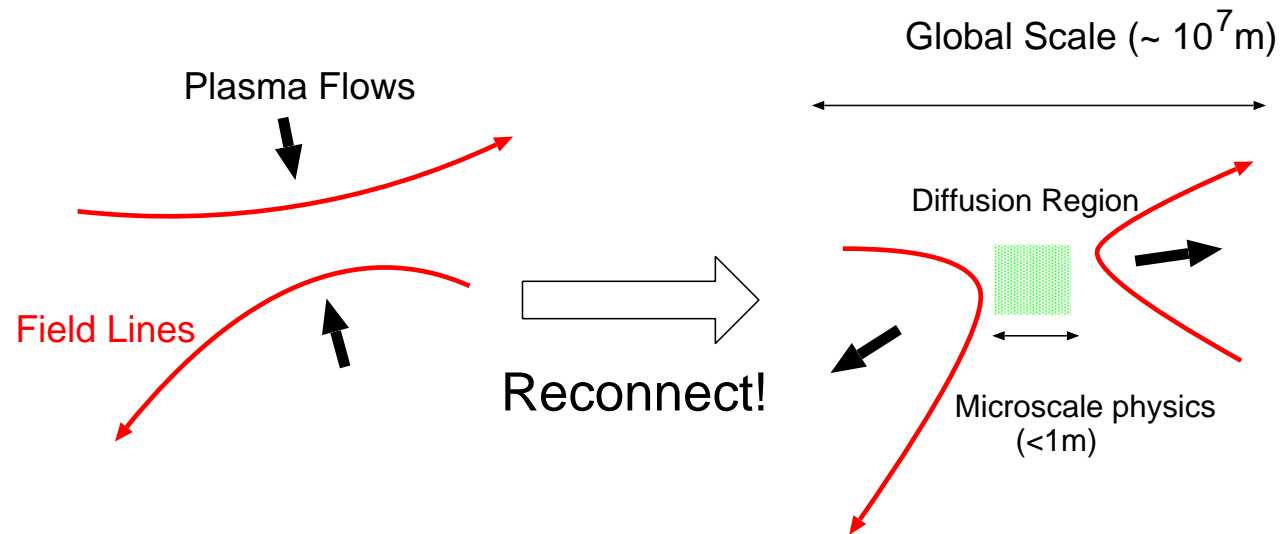
A) Center for Multiscale Plasma Dynamics, Univ. Maryland

B) Associação EURATOM/IST, Instituto de Plasmas e Fusão Nuclear

C) Dept. Phys. & Astron., Dartmouth College

D) Rudolf Peierls Centre for Theor. Phys., Univ. Oxford

Ubiquity of Magnetic Reconnection in Plasmas



- Magnetic reconnection converts magnetic field energy into high speed plasma flows, heating of plasmas, and energetic particles.
- Sawtooth oscillations, island growth due to tearing instabilities, disruptions in fusion experimental devices (Degradation of confinement).
- Magnetospheric substorms, solar, stellar flares in astrophysical situation.

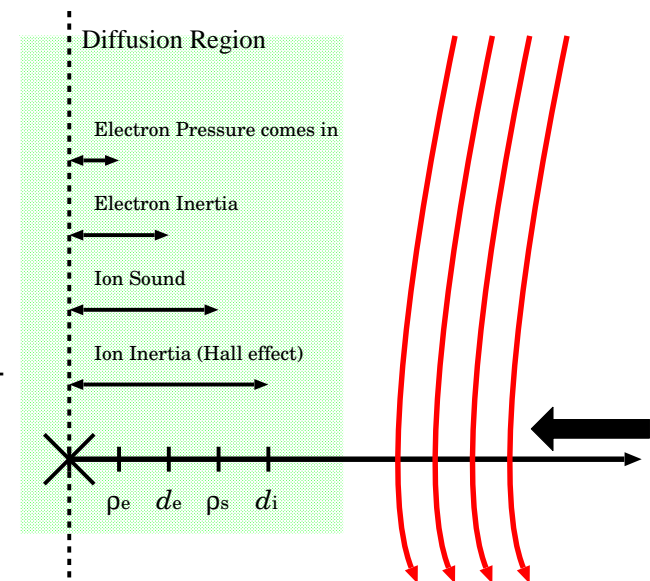
Magnetic Reconnection is Multiscale Problem

Magnetic reconnection is a classic example where multiple physics (scales) are involved

- Physics to break flux-freezing is necessary for field lines to change its topology: primarily by collisions (resistivity).
- In collisionless environments, time scale of reconnection based on resistivity is far too slow to explain realistic explosive phenomena.
- Resistive spatial scale falls below kinetic scales (MHD theory is not valid).
- Global structure drastically changes depending on microscopic processes.

Questions

- What determines time scale of reconnection?
- What provides mechanism for field lines to reconnect?
- What results? – Heating of electrons and/or ions? Electron jet flows? Islands? Transport in fusion devices?



Tearing Instability – Linear Theory

- Tearing instability is a resistive instability of current sheet configuration
- Spontaneous onset of reconnection process
- Standard boundary layer or singular perturbation problem

Since the pioneering work by Furth, Killeen, and Rosenbluth [PoF (1963)] based on MHD model, in which they derived the growth rate scaling $\gamma\tau_A \propto S^{-3/5}$, the linear tearing instability theory has been extended by including various non-MHD (kinetic) effects.

- **Hall effect** (Ion inertia)^a $\sim d_i$ – Alfvén wave dispersion (Whistler)
- **Pressure effect**^b (Ion Sound) $\sim \rho_s$ – Alfvén wave couples to sound wave
- Finite Larmor Radius (FLR)^c $\sim \rho_{i(e)}$ – Alfvén wave dispersion (KAW)
- Tensorial pressure $\sim \rho_{e(i)}$ – break flux-freezing
- **Electron inertia**^d $\sim d_e$ – break flux-freezing

^a e.g. Terasawa, GRL (1983), Fitzpatrick & Porcelli, PoP (2004)

^b Coppi *et al.*, NF (1966).

^c Porcelli, PRL (1991)

^d Schep *et al.*, PoP (1994)

Nonlinear Evolution of Tearing Mode

- Slow (algebraic) growth of island [Rutherford, PoF (1973)]: $dW/dt = \eta\Delta'$ where $W = 4\sqrt{\psi/\psi_0''}$ is the island width.
- X-point collapse and Sweet-Parker reconnection for $W > W_c \simeq 25/\Delta'$ [Waelbroeck, PRL (1993)]

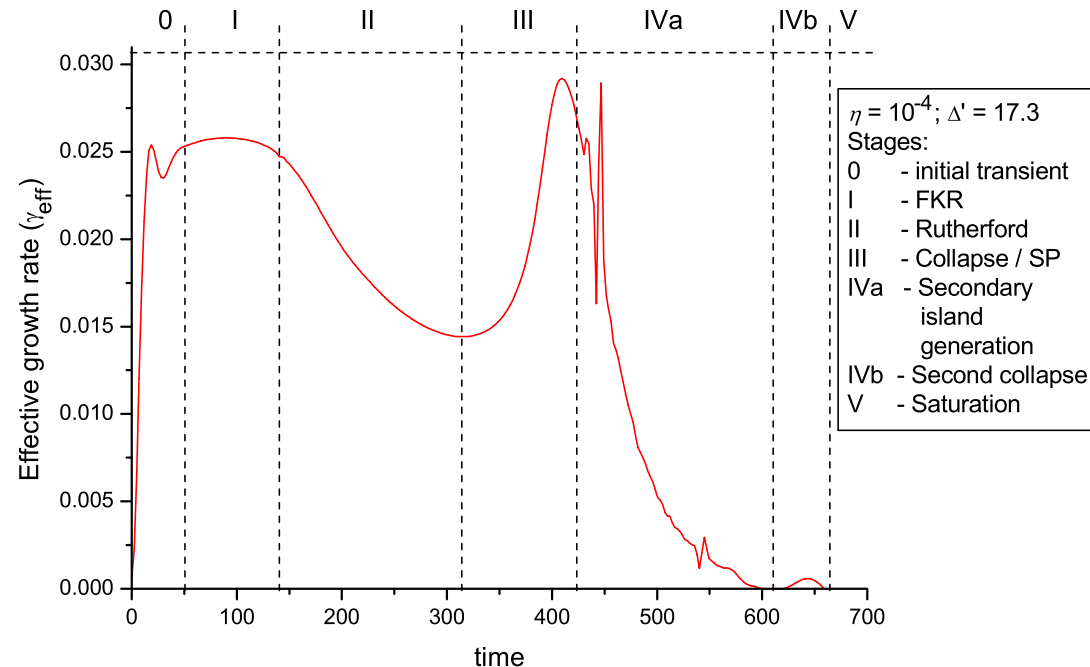
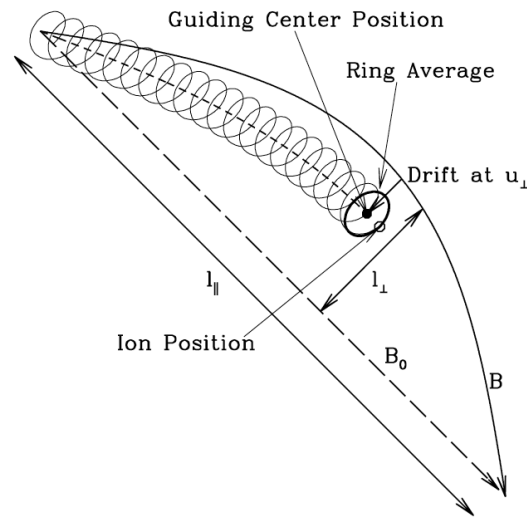


Figure illustrates regimes of tearing mode in MHD [image taken from Loureiro *et al.*, PRL (2005).]

Reduced Kinetic Approach to Multiscale Problem – Gyrokinetics



- Reduced kinetic model – 5 dimensional phase space.
- Existence of mean field (B_0) allows to separate out fast cyclotron motion – only low-frequency dynamics $\omega < \Omega_c$.
- Multiscale – distinct parallel and perpendicular scales ($k_{\parallel} \gg k_{\perp}$).
- Retains finite Larmor radius (FLR) effects, wave-particle interactions; orders out fast MHD waves, cyclotron resonance.
- Note: two-dimensional magnetic reconnection or tearing instability dynamics primarily independent of the guide magnetic field. (In the sense of simplest incompressible model.)

Gyrokinetics: Basic equations

The distribution function of particles is given by $f = \left(1 - \frac{q\phi}{T_0}\right) f_0 + h$, where $f_0 = n_0/(\sqrt{\pi}v_{\text{th}})^3 \exp(-v^2/v_{\text{th}}^2)$ is the Maxwellian, and the thermal velocity is given by $v_{\text{th}} = \sqrt{2T_0/m}$. The equations to solve are the gyrokinetic equation for $h = h(\mathbf{R}, V_{\perp}, V_{\parallel})$,

$$\frac{\partial h}{\partial t} + V_{\parallel} \frac{\partial h}{\partial Z} + \frac{1}{B_0} \{ \langle \chi \rangle_{\mathbf{R}}, h \} - \langle C(h) \rangle_{\mathbf{R}} = q \frac{f_0}{T_0} \frac{\partial \langle \chi \rangle_{\mathbf{R}}}{\partial t}, \quad (1)$$

$\chi = \phi - \mathbf{v} \cdot \mathbf{A}$ and the field equations for $\phi(\mathbf{r})$, $A_{\parallel}(\mathbf{r})$, and $\delta B_{\parallel}(\mathbf{r})$,

$$n_i = n_e \quad \Leftrightarrow \quad \sum_s \left[-\frac{q_s^2 n_{0s} \phi}{T_{0s}} + q_s \int \langle h_s \rangle_{\mathbf{r}} d\mathbf{v} \right] = 0,$$

$$(\nabla \times \mathbf{B})_{\parallel} = \mu_0 j_{\parallel} \quad \Leftrightarrow \quad \nabla_{\perp}^2 A_{\parallel} = -\mu_0 \sum_s q_s \int \langle h_s \rangle_{\mathbf{r}} v_{\parallel} d\mathbf{v}$$

$$\nabla \cdot \left(\mathbf{I} \frac{B_0 \delta B_{\parallel}}{\mu_0} + \mathbf{P} \right) = 0 \quad \Leftrightarrow \quad \frac{B_0}{\mu_0} \nabla_{\perp} \delta B_{\parallel} = -\nabla_{\perp} \cdot \sum_s \int \langle m \mathbf{V}_{\perp} \mathbf{V}_{\perp} h_s \rangle_{\mathbf{r}} d\mathbf{v}.$$

Gyrokinetics: Collision Operator

Recently, linearized collision operators for gyrokinetic simulations, which satisfies physical requirements are established and implemented in `AstroGK`^a.

The operators are the pitch-angle scattering (Lorentz), the energy diffusion, and moments conserving corrections to those operators for like-particle collisions. Electron-ion collisions consists of pitch angle scattering by background ions and ion drag are also included.

We, here, mainly discuss the electron-ion collisions since it contributes to resistivity. The operator is given by (in Fourier space)

$$C_{ei}(h_{e,\mathbf{k}}) = \nu_{ei} \left(\frac{v_{th,e}}{V} \right)^3 \left(\frac{1}{2} \frac{\partial}{\partial \xi} (1 - \xi^2) \frac{\partial h_{e,\mathbf{k}}}{\partial \xi} - \frac{1}{4} (1 + \xi^2) \frac{V^2}{v_{th,e}^2} k_{\perp}^2 \rho_e^2 h_{e,\mathbf{k}} + \frac{2V_{\parallel} J_0(\alpha_e) u_{\parallel,i,\mathbf{k}}}{v_{th,e}^2} f_{0e} \right) \quad (2)$$

We examine how this collision operator relates with resistivity which decays the current.

^a Abel *et al*, Phys. Plasmas **15**, 122509 (2008), arXiv:0808.1300; Barnes *et al*, Phys. Plasmas **16**, 072107 (2009), arXiv:0809.3945.

AstroGK reproduces Spitzer Resistivity

From the fluid picture current decays due to collisional resistivity as

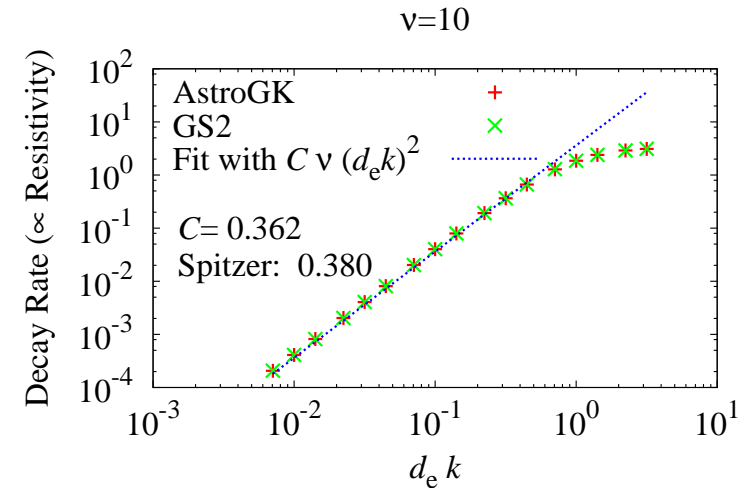
$$\frac{\partial j}{\partial t} = -\frac{\eta}{\mu_0} k^2 j, \quad (3)$$

and the decay rate is $\tau_{\text{decay}}^{-1} = (\eta/\mu_0)k^2$. Using the Spitzer resistivity given by $\eta = m_e/(1.98\tau_e n_e e^2)$ where $\tau_e = 3\sqrt{\pi}/(4\nu_{ei})$, the decay rate is casted into the following form,

$$\tau_{\text{decay}}^{-1} = C\nu_{ei}(d_e k)^2 \quad (4)$$

where the constant $C = 4/(1.98 \times 3\sqrt{\pi}) \approx 0.380$.

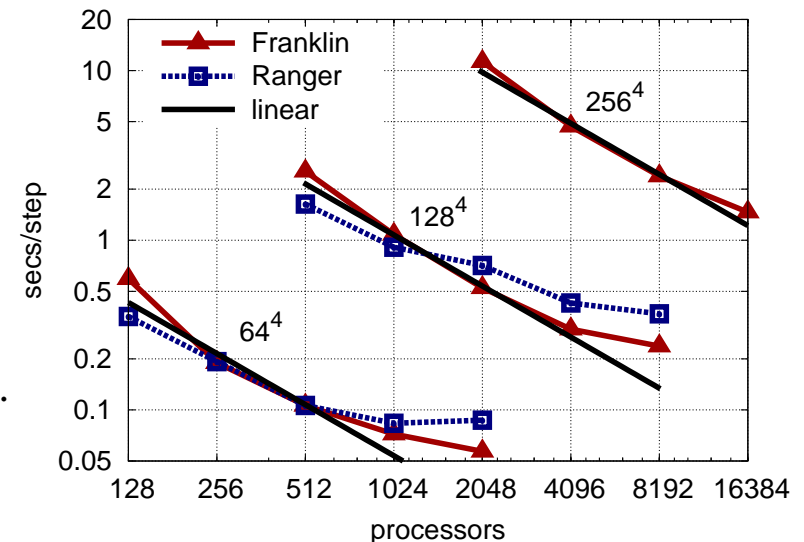
Figures show dependence of decay rate on ν and $d_e k$. Numerical estimated proportionality constant agrees with Spitzer's value within 5% error for $d_e k < 1$.



AstroGK Code Details

AstroGK is derived from GS2 by removing magnetic geometry effects to study fundamental aspects of kinetic plasmas mainly focusing on astrophysical problems. The code is publicly available at <https://sourceforge.net/projects/gyrokinetics/>. [E-Print: arXiv:1004.0279, submitted to JCP.]

- Eulerian continuum, local flux tube, δf , electromagnetic code.
- Fourier spectral in x and y .
- 2nd-order compact finite difference in z .
- Periodic boundary in x , y , and z .
- Gaussian quadrature for velocity space integral.
- Time integral:
 - 1st-order implicit scheme for all linear terms (including collisions).
 - 3rd-order Adams-Bashforth for nonlinear terms.
- Parallelized using MPI library – Scales up to ~ 10000 procs.
- Easy to port: works on laptop PCs to major scalar supercomputers, e.g. Jaguar @ NCCS (Cray XT4, 5), Ranger @ TACC (Sun Constellation Linux Cluster).



Simulation Setup

- Electron and one ion species, both treated kinetically.
- Purely 2D: $k_z = 0$.
- Equilibrium (on top of f_{0s} and B_{z0}): $\delta f_{e0} \propto v_{\parallel} f_{0e}$ such that

$$A_{\parallel 0}(x) = A_{\parallel 00} \cosh^{-2} \left(\frac{x - L_x/2}{a} \right) S_h(x), \quad B_{y0} = \partial_x A_{\parallel 0} \quad (5)$$

where $A_{\parallel 00}$ is a constant, a defines the typical scale length of the system, L_x is the box size, S_h is a shape function to enforce periodicity. ($S_h = 1$ in most of the region, and quickly falls to zero near the boundaries.) $\phi_0 = \delta B_{\parallel 0} = 0$, and $\delta f_{i0} = 0$.

- Perturbation: $k_y a = 0.8$ gives $\Delta' a \approx 23$.
- Energy source: We maintain the equilibrium $A_{\parallel 0}$ throughout the simulation. It is interpreted physically that energy is injected into the system to compensate the collisional energy loss.

Linear Tearing Instability: Problem Setup

Parameters

$$r \equiv \rho_S / a, \quad \sigma \equiv m_e / m_i, \quad (6)$$

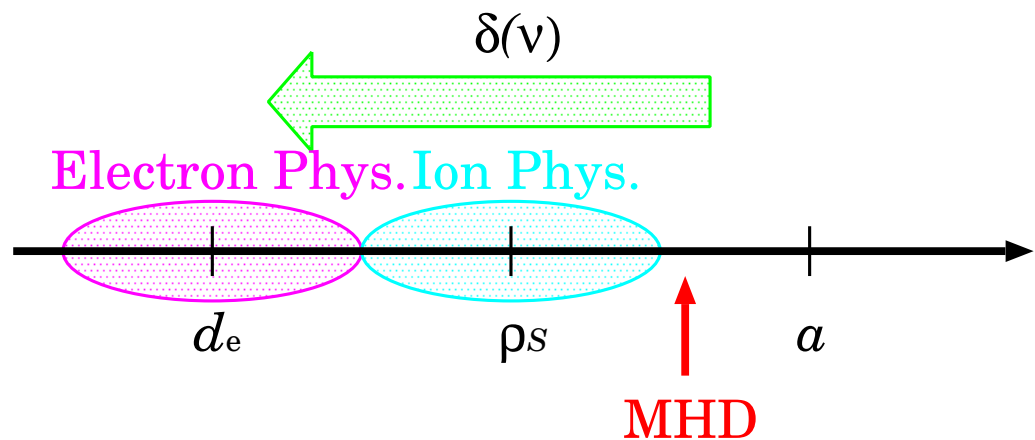
$$\tau \equiv T_{0i} / T_{0e}, \quad \beta_e \equiv n_0 T_{0e} / (B_0^2 / 2\mu_0) \quad (7)$$

$\rho_S \equiv \sqrt{T_{0e} / m_i} / \Omega_{ci}$ is the ion sound Larmor radius, B_0 is the guide magnetic field

$$\rho_i / \rho_S = \tau^{1/2}, \quad d_i / \rho_S = \beta_e^{-1/2}, \quad (8)$$

$$\rho_e / \rho_S = \sigma^{1/2}, \quad d_e / \rho_S = \beta_e^{-1/2} \sigma^{1/2}, \quad (9)$$

- Change collisionality ν to vary current layer width δ

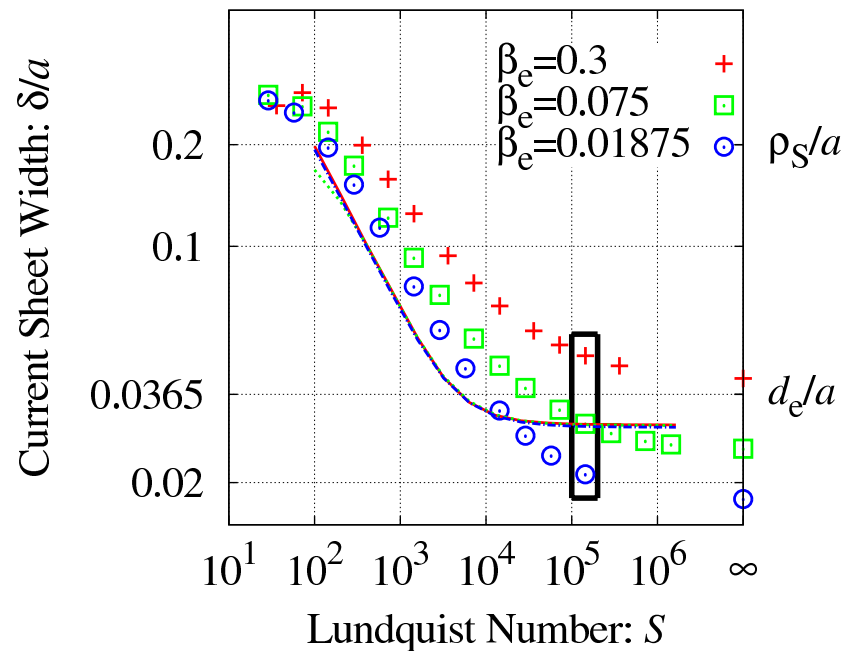
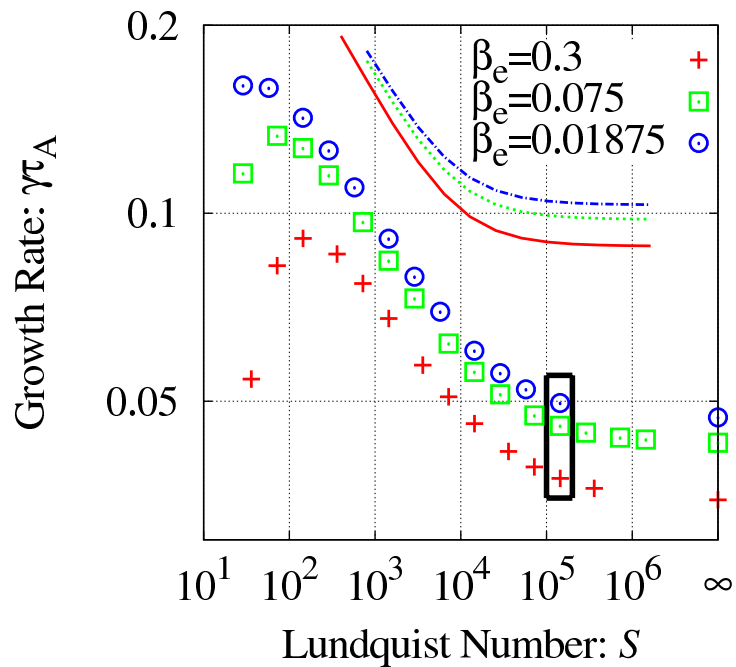
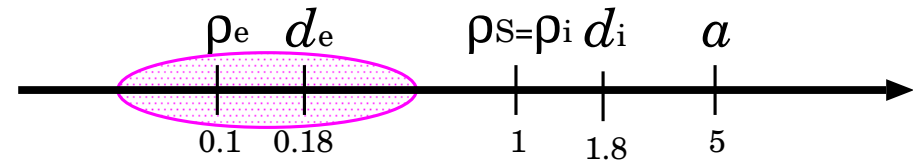


Collisional-Collisionless Transition

β_e and σ varied with fixed d_e

$$r = 0.2, \quad \tau = 1, \quad \sigma = 0.01, \quad \beta_e = 0.3$$

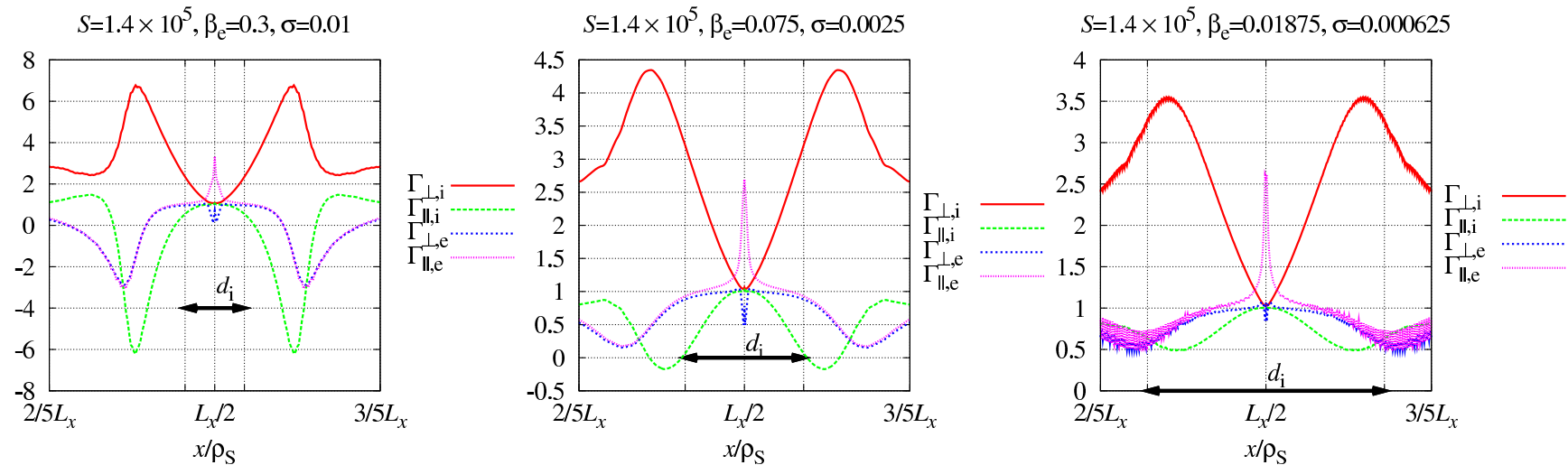
(10)



- Transition to collisionless reconnection – independent of collisions
- Electron inertia mediated – d_e sets lower bound of scale
- Difference with Hall RMHD (valid when $\tau \ll 1$) because of pressure treatment

Polytropic Eqn. of State is not Valid

Polytropic Eqn. of State $p \propto (n_0 m)^\Gamma$ leads to $\tilde{p} = \Gamma T_0 \tilde{n}$ or $\tilde{T}/T_0 = (\Gamma - 1)\tilde{n}/n_0$



- Direct measurements of $\Gamma_{\perp,\parallel}$ shows non-isotropy & non-polytropy
- Electrons temperature fluctuations are large inside the electron layer ($\sim d_e$) and zero outside the layer (far outside the layer both density and temperature is zero)

Energy Partition Diagnostics to Measure Linear Phase Mixing

FLR effects brings about a phase mixing effect which creates velocity space structures and then enhances collisional dissipation. To see this effect, we define the following energy quantities, and observe collisional dissipation.

Generalized gyrokinetic energy

$$W = \int \left[\sum_s \int \frac{T_{0s} \delta f_s^2}{2f_{0s}} d\mathbf{v} + \frac{|\nabla_{\perp} A_{\parallel}|^2 + \delta B_{\parallel}^2}{2\mu_0} \right] d\mathbf{r} \quad (11)$$

Evolutions of the perturbed energy ($\tilde{W} = W - W^{\text{eq}}$) is given by

$$\frac{d\tilde{W}}{dt} = P - D \quad (12)$$

where the input power P and dissipation D are given by

$$P = \int \frac{T_{0e} h_e}{f_{0e}} C(h_{e,0}) d\mathbf{v}, \quad D = \int \frac{T_{0e} h_e}{f_{0e}} C(h_e - h_{e,0}) d\mathbf{v}. \quad (13)$$

Is There Linear Phase Mixing? – No!

Fraction [%] of energy components and dissipation to P

Case A,B,C are collisionless $S = 1.4 \times 10^5$, varied β_e : A: $\beta_e = 0.3$, B: $\beta_e = 0.075$, C: $\beta_e = 0.01875$.

Case D, E are collisional with fixed $\beta_e = 0.3$: D: $S = 3.6 \times 10^3$, E: $S = 1.4 \times 10^2$, $\beta_e = 0.3$.

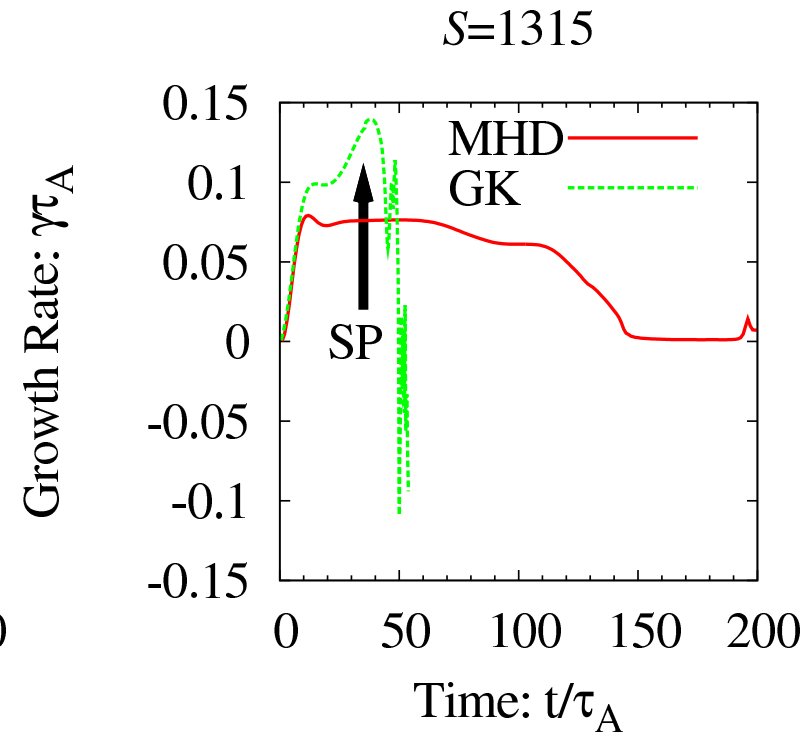
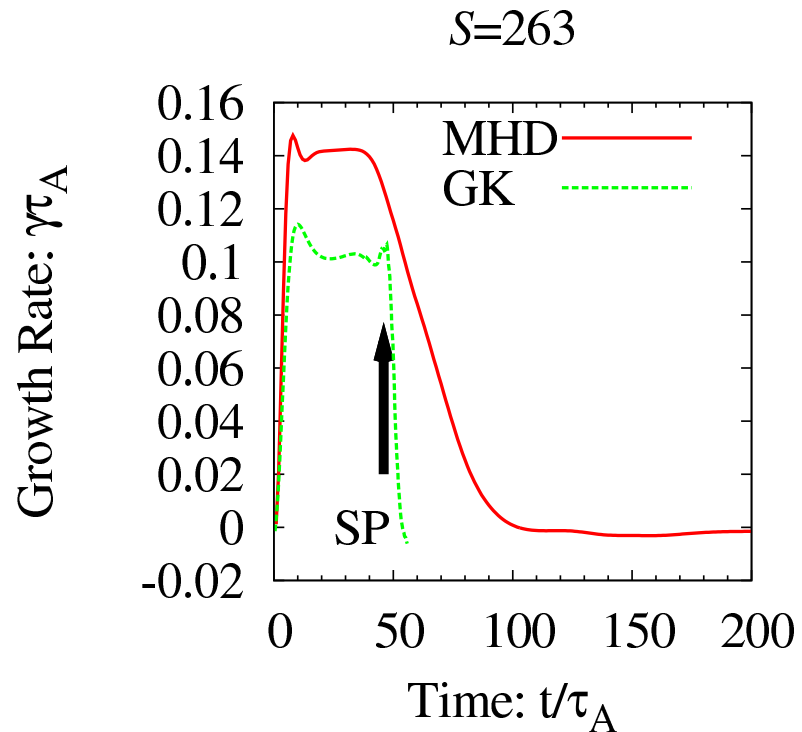
Case	$E_{K\perp,i}$	$E_{K\perp,e}$	$E_{K\parallel,i}$	$E_{K\parallel,e}$	$E_{T,i}$	$E_{T,e}$	$E_{M,\perp}$	$E_{M,\parallel}$	D
A	1.9	1.6	1.1	5.3	5.6	6.7	73.4	1.1	3.2
B	2.0	1.3	0.7	7.5	4.9	6.8	74.3	0.5	1.9
C	2.0	0.7	0.3	8.8	5.4	6.8	74.4	0.2	1.4
D	4.1	0.7	2.0	2.6	7.0	2.7	70.0	1.5	9.3
E	9.5	0.2	6.0	0.4	10.1	2.0	46.5	1.2	24.1

- Dissipation is weak in collisionless case.
- Fine velocity space structure does not develop. (As a result, the numbers of velocity grids of ~ 10 are sufficient.)
- Ballistic term (parallel phase mixing along the perturbed [in gyrokinetic sense] magnetic field) yields $\propto e^{iJ_0(k_\perp \rho_i)k_y B_{y0} v_\parallel t}$ dependence, whose time scale is slower than the tearing growth rate.

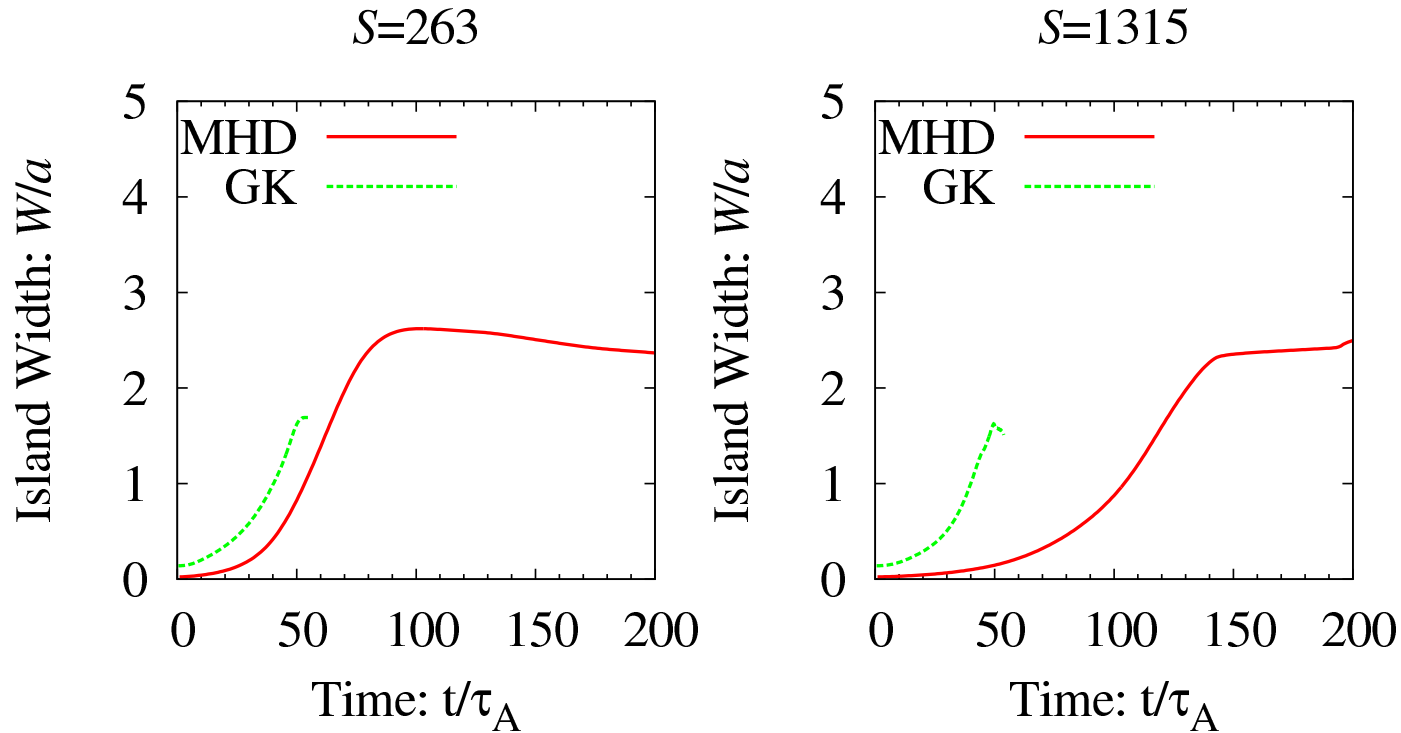
Nonlinear Stage: Only Low S So Far

$$r = \rho_S/a = 0.25, \quad \beta_e = 0.25, \quad m_i/m_e = 0.01, \quad T_{0i}/T_{0e} = 1 \quad (14)$$

$$\rho_i/a = \rho_S/a = 0.25, \quad d_i/a = 0.5, \quad d_e/a = 0.05, \quad \rho_e/a = 0.025. \quad (15)$$

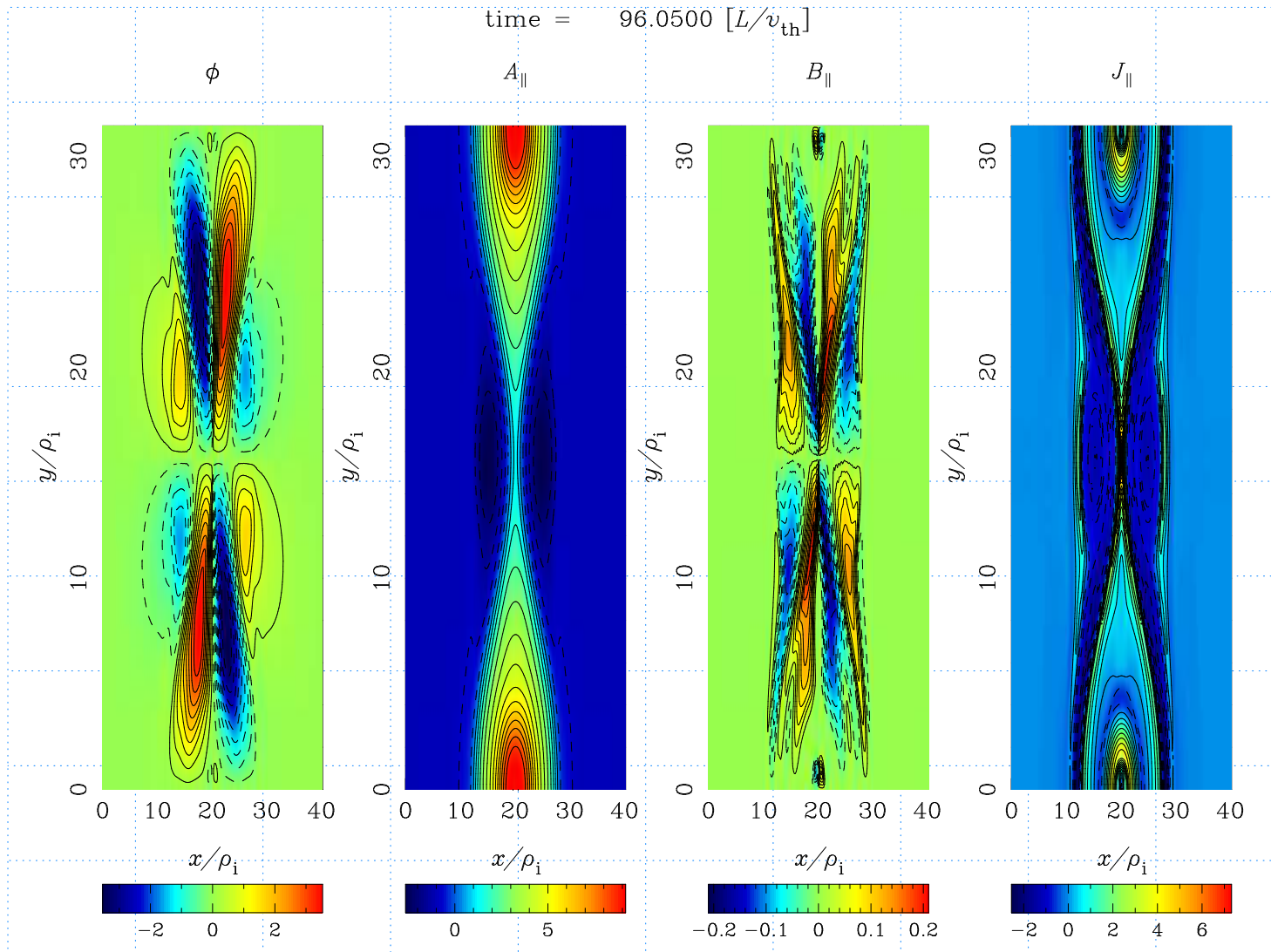


Nonlinear Stage: Island Growth and Saturation



- Smaller island width saturation level in GK compared with MHD.
- Critical island width for X point collapse is smaller in GK.
- ($S = 1315$ case may not be well resolved. Needs higher resolution.)

Nonlinear Stage



Summary

- Magnetic reconnection and tearing instability are very good example of multiscale physics.
- We have performed collisionless and collisional linear tearing instability simulations, and have scanned for ν_{ei} .
- We have observed transition from collisional regime (collision dependent growth rate) to collisionless regime (collision independent growth rate).
- Equation of state need to be considered carefully – not simply $p \propto \rho^\Gamma$
- Collisional dissipation and heating does not matter in linear regime
- We have also performed nonlinear simulations. Only small S so far. (Electron kinetic effects is minor.)
- Nonlinear tearing mode growth scenario has been confirmed in gyrokinetic simulations. X point collapse occurs even for small S case.
- Smaller island in gyrokinetic case. There may be other channels for energies to go: heating, kinetic energies.
- Further investigations are necessary: Detailed analysis for the stage after the collapse, e.g. scaling; What happens for collisionless case?

Acknowledged: CPMD, Leverhulme Trust Network, Wolfgang Pauli Inst., NERSC, NCCS, TeraGrid.